# 68Ga-PSMA–Guided Bone Biopsies for Molecular Diagnostics in Patients with Metastatic Prostate Cancer

Anouk C. de Jong*[1,2], Minke Smits*[3], Job van Riet[1,4], Jurgen J. Fütterer[5], Tessa Brabander[2], Paul Hamberg[6], Inge M. van Oort[7], Ronald de Wit[1], Martijn P. Lolkema[1], Niven Mehra[3], Marcel Segbers[†2], and Astrid A.M. van der Veldt[†1,2]

[1]Department of Medical Oncology, Erasmus MC Cancer Institute, Rotterdam, The Netherlands; [2]Department of Radiology and Nuclear Medicine, Erasmus MC, Rotterdam, The Netherlands; [3]Department of Medical Oncology, Radboud UMC, Nijmegen, The Netherlands; [4]Cancer Computational Biology Center, Erasmus MC Cancer Institute, Rotterdam, The Netherlands; [5]Department of Radiology and Nuclear Medicine, Radboud UMC, Nijmegen, The Netherlands; [6]Department of Internal Medicine, Franciscus Gasthuis and Vlietland, Rotterdam, The Netherlands; and [7]Department of Urology, Radboud UMC, Nijmegen, The Netherlands

For individual treatment decisions in patients with metastatic prostate cancer (mPC), molecular diagnostics are increasingly used. Bone metastases are frequently the only source for obtaining metastatic tumor tissue. However, the success rate of CT-guided bone biopsies for molecular analyses in mPC patients is approximately only 40%. PET using 68Ga prostate-specific membrane antigen (68Ga-PSMA) is a promising tool to improve the harvest rate of bone biopsies for molecular analyses. The aim of this study was to determine the success rate of 68Ga-PSMA–guided bone biopsies for molecular diagnostics in mPC patients. **Methods:** Within a prospective multicenter whole-genome sequencing trial (NCT01855477), 69 mPC patients underwent 68Ga-PSMA PET/CT before bone biopsy. The primary endpoint was the success rate (tumor percentage ≥ 30%) of 68Ga-PSMA–guided bone biopsies. At biopsy sites, 68Ga-PSMA uptake was quantified using rigid-body image registration of 68Ga-PSMA PET/CT and interventional CT. Actionable somatic alterations were identified. **Results:** The success rate of 68Ga-PSMA–guided biopsies for molecular analyses was 70%. At biopsy sites categorized as positive, inconclusive, or negative for 68Ga-PSMA uptake, 70%, 64%, and 36% of biopsies were tumor-positive (≥30%), respectively ($P = 0.0610$). In tumor-positive biopsies, 68Ga-PSMA uptake was significantly higher ($P = 0.008$), whereas radiodensity was significantly lower ($P = 0.006$). With an area under the curve of 0.84 and 0.70, both 68Ga-PSMA uptake ($SUV_{max}$) and radiodensity (mean Hounsfield units) were strong predictors for a positive biopsy. Actionable somatic alterations were detected in 73% of the sequenced biopsies. **Conclusion:** In patients with mPC, 68Ga-PSMA PET/CT improves the success rate of CT-guided bone biopsies for molecular analyses, thereby identifying actionable somatic alterations in more patients. Therefore, 68Ga-PSMA PET/CT may be considered for guidance of bone biopsies in both clinical practice and clinical trials.

**Key Words:** bone biopsy; 68Ga-PSMA-PET; molecular diagnostics; whole-genome sequencing; prostate cancer

With more than 350,000 men dying of prostate cancer in 2018, prostate cancer is not only one of the most common malignancies in men but also the fifth leading cause of cancer-related death worldwide (*1*). To improve treatment planning for individual patients with metastatic prostate cancer (mPC), molecular analyses are increasingly used to predict treatment response, guide clinical decision making, and identify additional targets for therapy (*2–4*). Because of tumor evolution and genetic adaption after castration resistance and subsequent treatment resistance, tumor DNA for molecular analyses is preferably obtained from a biopsy of a metastatic lesion. Because bone-only and bone-predominant disease are most frequently reported in patients with mPC, bone metastases are usually the only source for molecular analyses (*5,6*).

In men with mPC, 67%–77% of bone biopsies have sufficient quality for diagnostic histopathologic examination (*7–9*). However, molecular analyses on CT-guided bone biopsies from prostate cancer are less feasible, as the success rate is only 39%–44% and 36.5% for RNA analysis and whole-exome sequencing, respectively (*7,8,10*). This poor success rate of bone biopsies might be due to the predominantly osteoblastic character of these metastases. Because bone metastases of prostate cancer have a dense sclerotic matrix and decreased tumor cellularity, these lesions are difficult to distinguish from nonmalignant osteosclerosis on CT (*11*).

In clinical practice, most bone biopsies are guided by CT. Since the yield of CT-guided bone biopsies for molecular analyses is rather low, the use of molecular diagnostics for personalized treatment in prostate cancer patients is limited. To improve the yield of bone biopsies in mPC patients, biopsies could be obtained from bone metastases, which express prostate-specific membrane antigen (PSMA). In the apical region of normal prostate cells, PSMA shows physiologic expression, whereas it is usually 100–1,000× overexpressed in prostate cancer cells (*12*). To visualize and quantify PSMA expression in vivo, PET using 68Ga-PSMA can be performed. Nowadays, 68Ga-PSMA PET/CT is increasingly used in the setting of biochemical recurrence, as it has a high sensitivity and specificity for early detection of prostate cancer (*13*). Recently, fused images of 68Ga-PSMA PET/CT and diffusion-weighted MRI, in combination with cone-beam CT guidance, have been applied to guide bone biopsies in patients with prostate cancer. Although this pilot study was performed on only a small number of

patients ($n = 10$), it showed a success rate of 80% (*14*). Therefore, ^{68}Ga-PSMA PET/CT is a promising technique to increase the success rate of bone biopsies for molecular analyses in prostate cancer patients.

Within a prospective multicenter whole-genome sequencing (WGS) trial, we determined the success rate of ^{68}Ga-PSMA–guided bone biopsies for molecular diagnostics in mPC patients. In addition, we evaluated the potential impact of these molecular analyses on clinical decision making in mPC patients.

## MATERIALS AND METHODS

### Design

In this comprehensive PET study, mPC patients who had a ^{68}Ga-PSMA–guided bone biopsy within the prospective multicenter nationwide CPCT-02 study (NCT01855477) were included (*15*). CPCT-02 aims to improve selection of patients for experimental therapy by WGS of tumor DNA, which is obtained by image-guided biopsies. For the current study, informed consent was obtained within CPCT-02, and additional approval was provided by the institutional review boards of 2 academic institutes in The Netherlands: Erasmus Medical Center in Rotterdam and Radboud University Medical Center in Nijmegen.

### Patients

Between December 2014 and July 2018, all mPC patients who underwent ^{68}Ga-PSMA PET/CT within 12 wk before a completed bone biopsy procedure within CPCT-02 were included. The full inclusion and exclusion criteria of CPCT-02 were described previously (*15*). Tumor tissue was obtained from a metastatic lesion to fully capture the genomic tumor evolution. Patients could be included at multiple time points in their treatment course, resulting in repeated biopsies for some patients. Biopsies were always obtained before the start of a new systemic treatment. Clinical data were collected in an electronic case report form (ALEA Clinical).

### Primary and Secondary Endpoints

The primary endpoint was the success rate of ^{68}Ga-PSMA–guided bone biopsies in patients with mPC, with success defined as at least 30% tumor cells in at least 1 biopsy core (i.e., the minimal amount of tissue required for DNA isolation for WGS), as assessed by a dedicated pathologist. Exploratory endpoints included the correlation between biopsy success and imaging (SUV and Hounsfield units [HU]) and laboratory variables (hemoglobin, alkaline phosphatase, prostate-specific antigen, and lactate dehydrogenase). In addition, the potential impact of molecular analyses on clinical decision making was evaluated.

### Image Acquisition

Before the biopsy procedure, ^{68}Ga-PSMA PET/CT was performed to identify a biopsy site with high ^{68}Ga-PSMA uptake. During the procedure, biopsies were performed with or without CT, or ultrasound guidance, as decided by the interventional radiologist.

*[68]Ga-PSMA PET and Low-Dose CT.* On-site, PSMA-*N,N′*-bis [2-hydroxy-5-(carboxyethyl)benzyl]ethylenediamine-*N,N′*-diacetic acid was labeled with ^{68}Ga and administered intravenously with a mean (±SD) single bolus of $133 \pm 35$ MBq. At 60 min after injection, images were acquired from head to mid thigh on a Biograph mCT PET/CT scanner (Siemens Healthineers). A low-dose CT scan was acquired with 120 kV and 40 reference mAs (Erasmus Medical Center) or 50 reference mAs (Radboud University Medical Center). All PET data were obtained during 3 min per bed position, except for images with 4 min per bed position for patients weighing more than 70

kg at Erasmus Medical Center. For quantitative analyses of ^{68}Ga-PSMA uptake, data were reconstructed according to Evaluation and Report Language (*16*).

*Interventional CT.* Before CT acquisition for CT-guided biopsy, the field of view was determined by acquiring an overview image. Next, subsequent CT scans with a smaller field of view were acquired to visualize the biopsy needle until the biopsy site was reached.

### Biopsy Procedure

Bone biopsies were performed according to local institutional guidelines. The biopsy site was selected by the interventional radiologist based on clinical judgment, safety, and prior imaging, including ^{68}Ga-PSMA PET/CT.

### Image Analyses

*Rigid-Body Image Registration.* To evaluate whether biopsies were accurately obtained from a ^{68}Ga-PSMA–positive lesion, coregistration of ^{68}Ga-PSMA PET/CT and the interventional CT was retrospectively performed using rigid-body image registration. This analysis, which was performed with the Elastix Toolbox (*17,18*), enables measurement of ^{68}Ga-PSMA uptake at the exact position of the biopsy site. When the image quality of ^{68}Ga-PSMA PET, low-dose CT, and interventional CT was sufficient for rigid-body image registration, patients were included for this exploratory analysis. Rigid-body image registration merges ^{68}Ga-PSMA PET/CT and the interventional CT within 2 steps. To exclude soft tissues in both image registration steps, bone masks were obtained by applying a region-growing algorithm that included CT voxels greater than 150 HU. In the first coregistration step, patient motion on interventional CT was corrected by coregistration of the overview image and the image acquired during biopsy. Next, the overview image of the interventional CT was coregistered with the low-dose CT of the ^{68}Ga-PSMA PET/CT image. Combining rotation calculations from both image registration steps with interventional CT enabled fusion of ^{68}Ga-PSMA PET with the interventional CT, thereby visualizing the biopsy needle.

*[68]Ga-PSMA Uptake and Radiodensity at Biopsy Site.* An experienced nuclear medicine physician who did not know the biopsy results determined visually whether the biopsy was accurately taken from a ^{68}Ga-PSMA–positive lesion, using a 3-point scale categorized as hit, borderline, or miss. Besides these qualitative analyses, quantitative analyses consisted of SUV and HU measurements. To measure ^{68}Ga-PSMA uptake (SUV) and radiodensity (HU) at the exact biopsy location, a cylindric volume of interest with a length of 2 cm and a diameter of 1 cm was drawn at the site of the biopsy as visualized on rigid-body coregistration images of ^{68}Ga-PSMA PET and interventional CT. Volumes of interest were defined in Python using in-house–developed scripts, based on the SimpleITK framework for medical imaging (*19*). The $SUV_{max}$ and $SUV_{mean}$ of ^{68}Ga-PSMA uptake were calculated using the injected radioactivity, body weight, and amount of radioactivity within a volume of interest. To assess radiodensity in bone metastases, HU were determined on CT images. For CT measurements, if necessary, volumes of interest were minimally moved or reduced in size to avoid overlap with cortical bone.

### Molecular Analyses

Alterations in genes described in OncoKB, a precision oncology knowledge base, were extracted from the genomic data of all successfully sequenced biopsies and categorized as level 1, 2, 3, or 4 alterations, based on available clinical evidence (*20*). In addition, PTEN deletions were extracted because these might also be actionable with protein kinase B inhibitors (*2*).

*Processing and Analysis of WGS.* We requested the WGS data from the Hartwig Medical Foundation for prostate cancer patients (Erasmus MC and Radboud UMC) with bone metastasis who had successfully undergone a $^{68}$Ga-PSMA–guided biopsy and passed all pre- and post-WGS quality metrics ($n = 40$). These quality metrics consisted of a minimum tumor-cell percentage ($\geq$30%) as estimated by an expert pathologist, sufficient DNA yield, and an estimated in silico tumor-cell purity of at least 15%. Sample acquisition, library preparations, sequencing protocols, and processing (alignment, quality control, mutational calling, and others) were performed as part of the CPCT-02 study and have been described previously (*21,22*). In addition, GISTIC2 (version 2.0.23) (*23*) was performed to determine recurrent and high-level amplifications or deletions of chromosomal regions: gistic2 -b <output> -seg <segments> -refgene <hg19 UCSC> -genegistic 1 -gcm extreme -maxseg 4000 -broad 1 -brlen 0.98 -conf 0.95 -rx 0 -cap 3 - saveseg 0 -armpeel 1 -smallmem 0 -res 0.01 -ta 0.1 -td 0.1 -savedata 0 -savegene 1 -qvt 0.1.

Furthermore, we reannotated the somatic single-nucleotide, insertion/deletion, and multiple nucleotide variants with a variant-effect predictor using ENSEMBL annotations (ensembl-vep 95.1) (*24*) for GRCh37 and determined the overlap of genomic annotations based on GENCODE (version 30) (*25*) on copy-number alterations (GISTIC2) and structural variants. Per the somatic variant (at a nucleotide level), we selected the most deleterious coding effect per overlapping transcript; if a transcript had 2 or more coding mutations, these were summarized as "multiple mutations."

*Identification of Driver Genes and Clinically Actionable Somatic Events.* Potential driver genes were determined by unbiased selection using dndscv (0.0.1.0) (*26*), which detected genes under negative or positive mutational selection (qglobal_cv or qallsubs_cv $\leq$ 0.1) and by GISTIC2 (*23*) focal copynumber-peak discovery on cohortwide copy-number alterations (q $\leq$ 0.1) with GENCODE (version 30) annotations (*25*). This list of potential driver genes was complemented with detected driver genes based on the CPCT-02 pan-cancer study

(*21*). Structural variants potentially leading to known gene fusions involving TMPRSS2, ETV, ERG, or FLI1 were summarized as ETS fusions.

Somatic events (coding mutations, MSI, deep gain/deletions, and structural variants) were reviewed in OncoKB (*20*) (version of June 21, 2019) to assess any clinically actionable events. All molecular analyses were performed with the statistical language platform R (version 3.6.1) (*27*).

## Statistical Analyses

Depending on normality distribution, the unpaired *t* test or Mann–Whitney *U* test was used to test for differences between clinical variables (age, Gleason score, hemoglobin, alkaline phosphatase, lactate dehydrogenase, and prostate-specific antigen), imaging variables ($HU_{mean}$, $HU_{max}$, $SUV_{mean}$, and $SUV_{max}$), and primary outcome of biopsy ($\geq$30% tumor). To test for differences between the summed Gleason score ($<8$ and $\geq8$) and primary outcome, a $\chi^2$ test was used. The 3 $^{68}$Ga-PSMA uptake categories (hit, borderline, and miss) were compared for tumor positivity ($\geq$30% tumor) using the $\chi^2$-for-trend test. For SUV at the biopsy location, the 3 biopsy outcome groups were compared using the Kruskal–Wallis test in combination with the Dunn multiple-comparisons test. Univariate and multivariate regression analyses were performed to evaluate relations between variables and primary outcome. For these analyses, all nonnormally distributed variables were log-transformed before testing. Since a normal distribution was not reached for lactate dehydrogenase by log transformation, lactate dehydrogenase was categorized as normal ($<250$) or elevated ($\geq250$) and a $\chi^2$ test was used to test for an association with biopsy outcome. Univariate logistic regression analysis tested for any association between continuous variables and primary outcome. Subsequently, significantly associated variables were selected for multivariate logistic regression analysis. Because of the relatively small sample size, the most significant variables of HU (mean or maximum) and SUV (mean or maximum) were selected for multivariate testing. No correction was set for multiplicity of secondary endpoints. The odds for a positive biopsy were calculated by logistic regression for SUV and HU. For the area under the curve and receiver-operating-characteristic curve, the logarithm of odds was calculated. Receiver-toperating-characteristic curves were calculated for $HU_{mean}$ and $SUV_{max}$. All statistical tests were performed 2-sided. A *P* value of no more than 0.05 was considered statistically significant.

## RESULTS

### Biopsy Selection

Between December 2014 and June 2018, 115 bone biopsies from 103 patients with mPC were obtained within CPCT-02 at Erasmus Medical Center and Radboud University Medical Center. For 71 biopsies (62%), $^{68}$Ga-PSMA PET/CT was performed beforehand to identify bone metastases, whereas 44 biopsies (38%) within CPCT-02 were preceded by other imaging modalities. Two of 71 $^{68}$Ga-PSMA–guided biopsies (3%) were not eligible because of a failed biopsy procedure and an interval of more than 12 wk between imaging and
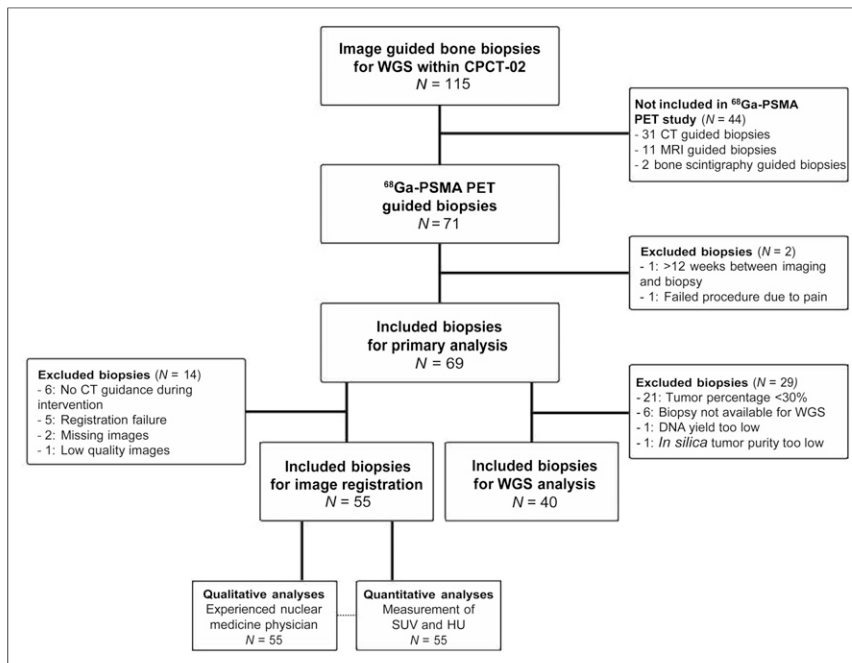


**FIGURE 1.** Flowchart of included $^{68}$Ga-PSMA–guided bone biopsies for primary and secondary analyses of current PET study within CPCT-02.

biopsy. In total, 69 $^{68}$Ga-PSMA–guided biopsies, from 60 individual patients, were eligible for primary analysis to determine the success rate of $^{68}$Ga-PSMA–guided bone biopsies (Fig. 1). Seven patients underwent 2 $^{68}$Ga-PSMA–guided bone biopsies, and 1 patient underwent 3 $^{68}$Ga-PSMA–guided bone biopsies. The median time between $^{68}$Ga-PSMA PET/CT and the biopsy procedure was 9 d (interquartile range [IQR], 3–22 d).

### Clinical Characteristics and Success Rate of $^{68}$Ga-PSMA– Guided Biopsies

The clinical characteristics of patients and biopsies are described in Table 1. Biopsies were performed primarily in the castration-resistant setting (97%, $n = 67$) and most commonly were obtained from the pelvis ($n = 57$, 83%). During the procedure, biopsies were performed unguided ($n = 5$, 7%) or guided by ultrasound ($n = 1$, 1%) or CT ($n = 63$, 91%), as decided by the interventional radiologist. During 1 biopsy procedure (1%), excessive bleeding, which was directly controlled by manual pressure, occurred.

On the basis of tumor percentage ($\geq$30%) in at least 1 core, 48 of 69 (70%) $^{68}$Ga-PSMA–guided biopsies (44/60 individual patients [73%]) were eligible for molecular analyses. No significant differences were found in age ($P = 0.42$), Gleason score ($P = 0.46$), or baseline laboratory findings (hemoglobin, $P = 0.54$; prostate-specific antigen, $P = 0.36$; alkaline phosphatase, $P = 0.56$) between biopsies with tumor percentage of 30% or less and tumor percentage of 30% or more, although elevated lactate dehydrogenase levels were seen with borderline significance in the group with a successful biopsy ($P = 0.05$). In the univariate logistic regression analysis, none of these variables were associated with biopsy outcome. The success rate of biopsies obtained from pelvis ($n = 57$, 83%), spine ($n = 6$, 9%), and other locations ($n = 6$, 9%) was 65%, 100%, and 83%, respectively.

### $^{68}$Ga-PSMA Uptake and Radiodensity at Biopsy Site

To evaluate whether biopsies were accurately obtained from lesions with high $^{68}$Ga-PSMA uptake, $^{68}$Ga-PSMA PET/CT was coregistered with interventional CT (Figs. 2A–2D) for qualitative and quantitative analyses (Fig. 1). For 55 biopsies, rigid-body image registration could be performed adequately (Fig. 1). On the basis of the rigid-body image registrations, 33 biopsies were categorized as hit, 11 biopsies as borderline, and 11 biopsies as miss (Fig. 3A). As expected, biopsy sites categorized as hit had a higher SUV$_{max}$ and SUV$_{mean}$ than biopsy sites categorized as miss ($P < 0.001$ for both) (Figs. 3B and 3C). Subsequently, the correlation between $^{68}$Ga-PSMA uptake and biopsy outcome was evaluated. At biopsy sites categorized as hit, borderline, or miss for $^{68}$Ga-PSMA uptake, 70%, 64%, and 36% of biopsies were tumor-positive ($\geq$30%), respectively ($P = 0.0610$, Fig. 3A).

At biopsy sites with tumor percentage of 30% or more, median $^{68}$Ga-PSMA uptake was significantly higher (SUV$_{max}$, 20.9 [IQR, 10.0–32.1]; SUV$_{mean}$, 10.3 [IQR, 3.4–18.7]), whereas median $^{68}$Ga-PSMA uptake was lower at biopsy sites with tumor percentage of 30% or less (SUV$_{max}$, 6.7 [IQR, 3.7–14.2]; SUV$_{mean}$, 3.4 [IQR, 1.8–9.1]; $P = 0.0021$ and $P = 0.0123$, respectively) (Figs. 4A and 4B). In contrast, median radiodensity on CT was significantly lower at biopsy sites with tumor percentage of 30% or more (HU$_{max}$, 786 [IQR, 600–977]; HU$_{mean}$, 294 [IQR, 184–473]) than at biopsy sites with tumor percentage of 30% or less (HU$_{max}$, 1,019 [IQR, 780–1,132]; HU$_{mean}$, 524 [IQR, 296–738]; $P = 0.0266$ and

$P = 0.0064$, respectively) (Figs. 4C and 4D). In univariate logistic regression analysis, SUV and HU were also significantly associated with biopsy outcome (SUV$_{max}$, $P = 0.008$, SUV$_{mean}$, $P = 0.016$, HU$_{mean}$, $P = 0.006$, and HU$_{max}$, $P = 0.037$) (Supplemental Table 1A;

### TABLE 1
Clinical Characteristics at Time of $^{68}$Ga-PSMA–Guided Bone Biopsy

| Characteristic | Data |
| --- | --- |
| Location of bone biopsy | |
| Pelvis | 57 (82.6%) |
| Spine | 6 (8.7%) |
| Rib | 3 (4.3%) |
| Extremity | 3 (4.3%) |
| Location of bone biopsy irradiated | 3 (4.3%) |
| Age at biopsy (y) | 68.5 ± 8.3 |
| Gleason score at primary diagnosis | |
| 8 | 22 (31.9%) |
| ≥8 | 39 (56.5%) |
| Unknown | 8 (11.6%) |
| Prior local treatment | |
| Radical prostatectomy | 15 (21.7%) |
| External radiotherapy of prostate | 16 (32.2%) |
| Brachytherapy | 1 (1.4%) |
| Hormone status at time of biopsy | |
| mHSPC | 2 (2.9%) |
| mCRPC | 67 (97.1%) |
| Prior second-generation ADT | |
| Abiraterone | 23 (33.3%) |
| Enzalutamide | 34 (49.2%) |
| Prior chemotherapy | |
| Docetaxel | 49 (71%) |
| Cabazitaxel | 19 (27.5%) |
| Estramustine | 1 (1.4%) |
| Prior radiotherapy | |
| $^{223}$Ra | 5 (7.2%) |
| External radiotherapy of metastatic site | 21 (30.4%) |
| Laboratory values at time of biopsy | |
| Hemoglobin (mmol/L) ($n = 67$) | 8.0 (5.3–9.5) |
| Leukocytes (×10$^9$/L) ($n = 62$) | 6.5 (3.6–13.2) |
| Thrombocytes (×10$^9$/L) ($n = 65$) | 232 (122–576) |
| Alkaline phosphatase (U/L) ($n = 59$) | 123 (43–4,598) |
| LDH (U/L) ($n = 53$) | 233 (152–2,718) |
| PSA (μg/L) ($n = 63$) | 96 (0.14–2,375) |

mHSPC = metastatic hormone sensitive prostate cancer; mCRPC = metastatic castration-resistant prostate cancer; ADT = androgen deprivation therapy; LDH = lactate dehydrogenase; PSA = prostate-specific antigen.

Qualitative data are numbers followed by percentages in parentheses; continuous data are median followed by range in parentheses or mean ± SD.
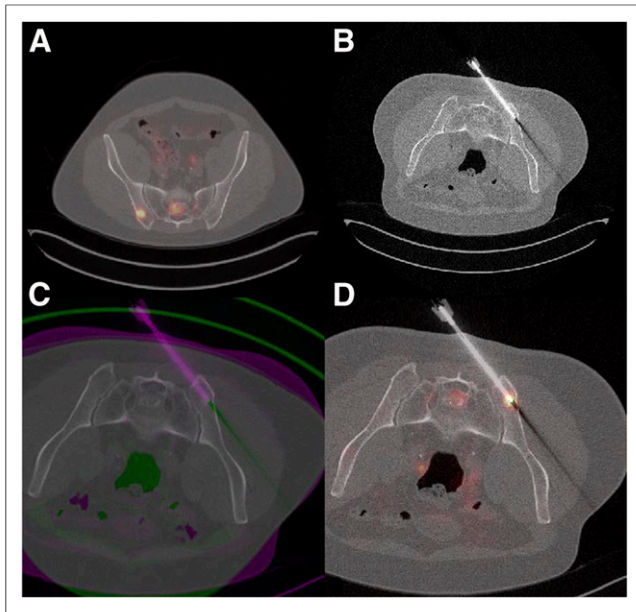
**FIGURE 2.** Rigid-body image registration of $^{68}$Ga-PSMA PET/CT and interventional CT visualizes biopsy needle on $^{68}$Ga-PSMA PET and enables measurement of $^{68}$Ga-PSMA uptake and radiodensity at biopsy site. (A) $^{68}$Ga-PSMA PET/CT, before biopsy. (B) CT, acquired during biopsy procedure. (C) Coregistration of $^{68}$Ga-PSMA PET/CT and interventional CT. (D) Visualization of biopsy needle on $^{68}$Ga-PSMA PET/CT.

supplemental materials are available at http://jnm.snmjournals.org). After stepwise multivariate analysis, $HU_{mean}$ and $SUV_{max}$ resulted in an odds ratio of 0.995 (95% confidence interval, 0.992–0.998; $P = 0.003$) and 11.737 (95% confidence interval, 2.258–60.996; $P = 0.003$), respectively (Supplemental Table 1B). The receiver-operating-characteristic curves of $HU_{mean}$ and $SUV_{max}$ for successful biopsies

had an area under the curve of 0.70 and 0.84, respectively (Supplemental Fig. 1).

### Clinical Impact of $^{68}$Ga-PSMA–Guided Bone Biopsies for Molecular Analyses

Forty of 48 positive biopsies (83%) were successfully used for WGS (Fig. 1). The median in silico tumor purity of the successfully sequenced samples was 55% (range, 17%–94%) (Supplemental Fig. 2) (20–27). In total, 53 actionable somatic alterations were detected in 73% ($n = 29$) of the successfully sequenced biopsies (Fig. 5). Forty-one actionable somatic alterations, detected in 21 biopsies, were described in the OncoKB database as level 1 ($n = 9$, 22%), level 2 ($n = 4$, 10%), level 3 ($n = 13$, 32%), or level 4 ($n = 15$, 37%) (20). Twelve biopsies (30%) contained a deep PTEN deletion, which is not (yet) included in the OncoKB database but might be actionable with protein kinase B inhibitors (2). The genomic landscape of metastatic castration-resistant prostate cancer, including this subset of biopsies, has been described in detail by van Dessel et al. (22).

### DISCUSSION

In this comprehensive PET study, we showed that 70% of $^{68}$Ga-PSMA–guided bone biopsies provide sufficient quality for molecular analyses. Our findings indicate that $^{68}$Ga-PSMA–guided bone biopsies are more successful than bone biopsies with CT guidance only, which have a reported success rate for molecular analysis of only 36.5%–44% in patients with mPC (7,8,10). With 70% of the biopsies being successful for molecular analyses, the success rate approximates the overall success rate of 76.5% for 3,655 biopsies within the CPCT-02 study, which included mainly nonskeletal biopsies (21).

For objective analyses of the success rate of $^{68}$Ga-PSMA–guided bone biopsies, we applied rigid-body image registration, which confirmed that most biopsies were accurately obtained from a lesion with high $^{68}$Ga-PSMA uptake. In addition, there was a trend toward a higher percentage of tumor-positive biopsies in the hit group. For biopsies with tumor percentage of 30% or more, $^{68}$Ga-PSMA uptake was significantly higher than for biopsies with tumor percentage of 30% or less. In contrast, HU on CT were lower for biopsies with tumor percentage of 30% or more than for biopsies with tumor percentage of 30% or less. The higher success rate of biopsies from bone lesions with lower HU has also been reported by 2 other studies (7,8), indicating that osteosclerotic lesions with high HU contain fewer viable tumor cells. With an area under the curve of 0.84 and 0.70, both $SUV_{max}$ and $HU_{mean}$ were strong predictors for a positive biopsy. In the absence of $^{68}$Ga-PSMA PET/CT, it might therefore be advisable to obtain biopsies from less sclerotic lesions with lower HU.

The high frequency of actionable alterations found in this study emphasizes the medical need for a high success rate of bone biopsies. Within the CPCT-02 trial, potentially actionable alterations, identified by WGS of
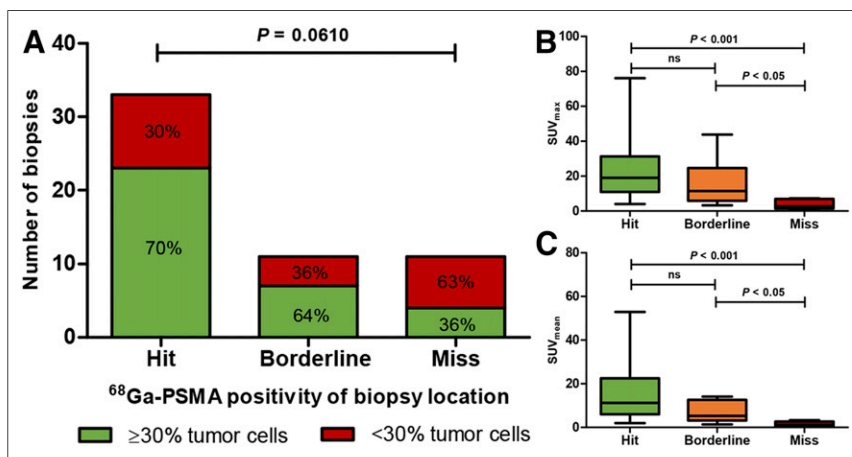


**FIGURE 3.** $^{68}$Ga-PSMA uptake at biopsy sites. (A) Biopsy sites were categorized as hit ($^{68}$Ga-PSMA–positive), borderline, or miss ($^{68}$Ga-PSMA–negative) by masked nuclear medicine physician and correlated to tumor percentage (≥30% vs. <30%). There were 55 biopsies, and χ² for trend test was performed. (B) $SUV_{max}$ at biopsy site, categorized by $^{68}$Ga-PSMA uptake score. There were 55 biopsies, and Kruskal–Wallis was performed in combination with Dunn multiple-comparisons test. (C) $SUV_{mean}$ at biopsy site, categorized by $^{68}$Ga-PSMA uptake score. There were 55 biopsies, and Kruskal–Wallis was performed in combination with Dunn multiple-comparisons test. ns = not statistically significant.
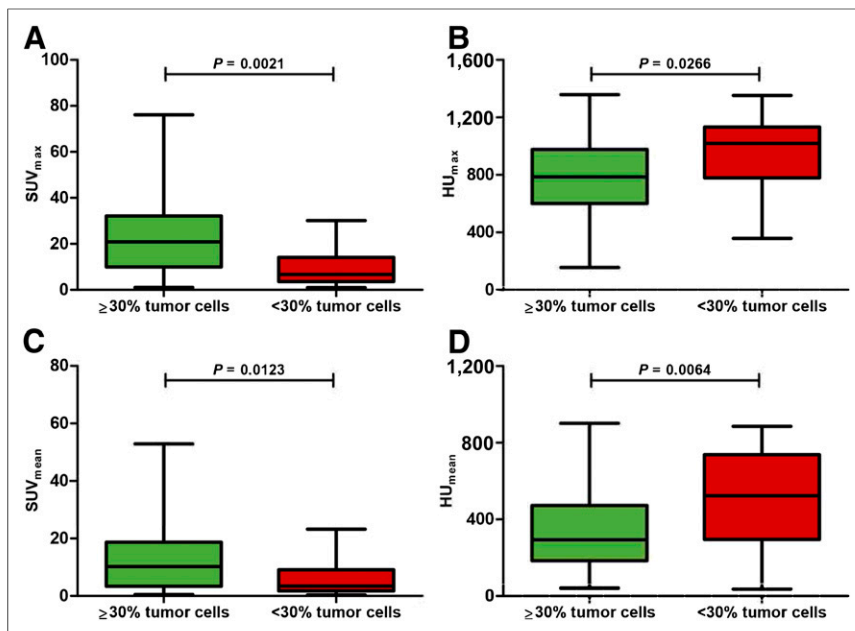
**FIGURE 4.** $^{68}$Ga-PSMA uptake (SUV) and radiodensity (HU) in biopsies with tumor percentage ≥ 30% and < 30%: $SUV_{max}$ (A), $SUV_{mean}$ (B), $HU_{max}$ (C), and $HU_{mean}$ (D). There were 55 biopsies, and Mann–Whitney test was performed for all parameters.

with approved, off-label targeted agents based on the molecular characteristics of the tumor. First results are promising, with clinical benefit for multiple treatment cohorts (28).

Because $^{68}$Ga-PSMA PET is becoming increasingly widely available in current clinical practice, it can easily be implemented to improve the success rate of bone biopsies. By optimizing the first step of the pipeline for molecular diagnostics, $^{68}$Ga-PSMA PET significantly contributes to improved genomic characterization of mPC.

Although the current study showed a high success rate, there are a few limitations of $^{68}$Ga-PSMA–guided bone biopsies for molecular diagnostics. First, tumor heterogeneity might be better reflected by molecular analyses of liquid biopsies than by WGS of tumor tissue from a single lesion. However, techniques for detailed molecular analyses of liquid biopsies are still under development, whereas WGS of tissue biopsies is currently more feasible. Second, PSMA expression has high inter- and intrapatient heterogeneity (29). High PSMA expression is associated with defective DNA damage repair and PTEN loss, whereas patients with low $^{68}$Ga-PSMA expression have poor survival (29–31). Since bone biopsies in this study were not obtained from metastases with low
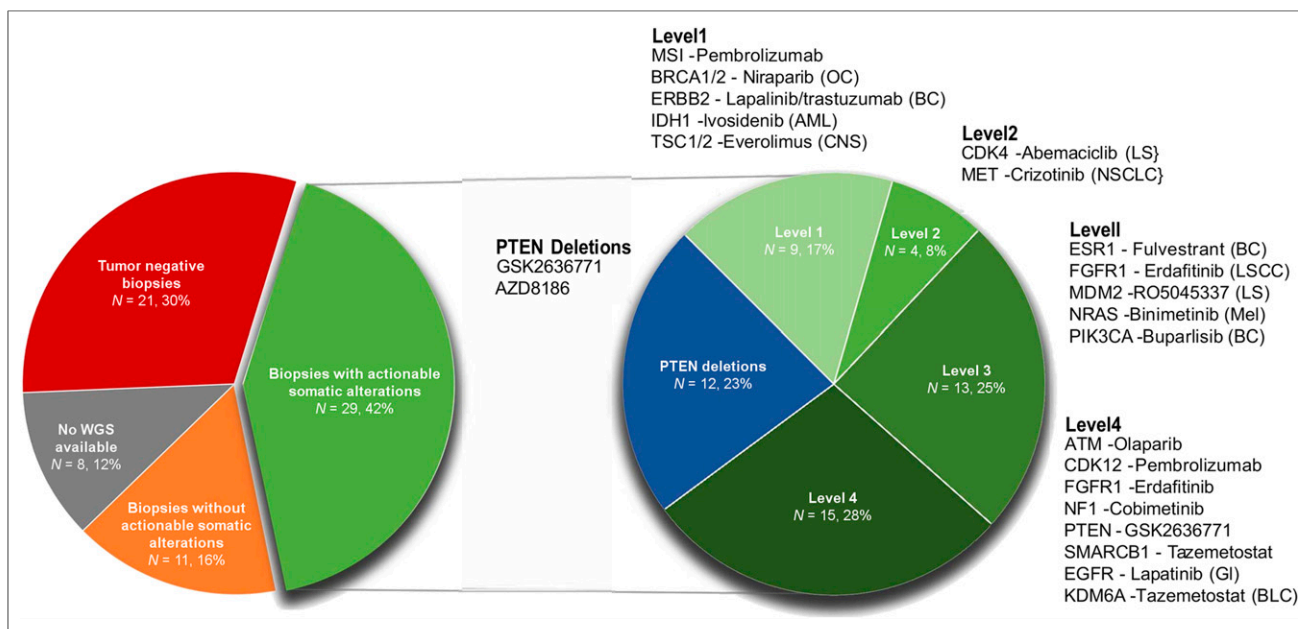
the tumor biopsy, were shared with the patient to enable targeted treatment in, for example, the Drug Rediscovery Protocol (NCT02925234). According to this protocol, patients are treated



**FIGURE 5.** Actionable somatic alterations, detected by WGS, in $^{68}$Ga-PSMA PET–guided bone biopsies from mPC patients. Genes with actionable somatic alterations are categorized by level of evidence for targeted therapy as described in OncoKB database. Evidence for both prostate cancer and other malignancies was combined within 1 category. Level 1: Food and Drug Administration (FDA)–recognized biomarker predictive of response to FDA-approved drug. Level 2: Standard-care biomarker predictive of response to FDA-approved drug. Level 3: Compelling clinical evidence supporting biomarker as being predictive of response to drug. Level 4: Compelling biologic evidence supporting biomarker as being predictive of response to drug. For every altered gene, example of targeted therapy suitable for specific alteration was described. AML = acute myeloid leukemia; BC = breast cancer; BLC = bladder cancer; CNS = central nervous system cancer; GI = glioma; LS = liposarcoma; LSCC = lung squamous cell carcinoma; Mel = melanoma; NSCLC = non–small cell lung cancer; OC = ovarian cancer.

<sup>68</sup>Ga-PSMA uptake, these sites are underrepresented in the current study.

In addition, there were some notable results. First, 4 biopsies that were scored as miss ($^{68}$Ga-PSMA–negative) did contain at least 30% tumor cells (false-negative). As these biopsies were all close to a $^{68}$Ga-PSMA–positive lesion, these false-negative results may be due to patients' movements or a difference in spatial resolution between scans. Although most biopsies were accurately obtained from lesions with high $^{68}$Ga-PSMA uptake, guidance might be further optimized by real-time visualization of $^{68}$Ga-PSMA uptake, though this is technically and logistically more challenging.

Second, in 5 biopsies, all of which were obtained from spine or ribs, image registration failed. This image registration failure at nonpelvic sites may be explained by the rigid-body algorithm, which relies on the assumption that the spine and rib cage are rigid bodies. As the rigid-body algorithm was applied only for image analyses in this study, this limitation will not impact the feasibility of $^{68}$Ga-PSMA–guided biopsies from nonpelvic sites in clinical practice.

## CONCLUSION

$^{68}$Ga-PSMA–guided bone biopsies have a 70% success rate for molecular analyses in mPC patients, indicating that $^{68}$Ga-PSMA PET/CT has added value to increase the success rate of CT-guided bone biopsies. In successful $^{68}$Ga-PSMA–guided biopsies, WGS identified numerous targetable mutations, emphasizing the potential clinical impact of $^{68}$Ga-PSMA–guided bone biopsies in mPC patients.

## DISCLOSURE

## ACKNOWLEDGMENTS

---

**KEY POINTS**

**QUESTION:** What is the success rate of $^{68}$Ga-PSMA–guided bone biopsies for molecular analyses in mPC patients?

**PERTINENT FINDINGS:** In 69 mPC patients who underwent $^{68}$Ga-PSMA PET/CT before bone biopsy within a prospective multicenter WGS trial (NCT01855477), the success rate of $^{68}$Ga-PSMA–guided bone biopsies for molecular analyses was 70%.

**IMPLICATIONS FOR PATIENT CARE:** In patients with mPC, $^{68}$Ga-PSMA PET/CT improves the success rate of CT-guided bone biopsies for molecular analyses, thereby identifying actionable somatic alterations in more patients.

## REFERENCES

1. Bray F, Ferlay J, Soerjomataram I, Siegel RL, Torre LA, Jemal A. Global cancer statistics 2018: GLOBOCAN estimates of incidence and mortality worldwide for 36 cancers in 185 countries. *CA Cancer J Clin.* 2018;68:394–424.

2. de Bono JS, De Giorgi U, Rodrigues DN, et al. Randomized phase II study evaluating AKT blockade with ipatasertib, in combination with abiraterone, in patients with metastatic prostate cancer with and without PTEN loss. *Clin Cancer Res.* 2019;25:928–936.

3. Mateo J, Carreira S, Sandhu S, et al. DNA-repair defects and olaparib in metastatic prostate cancer. *N Engl J Med.* 2015;373:1697–1708.

4. Abida W, Cheng ML, Armenia J, et al. Analysis of the prevalence of microsatellite instability in prostate cancer and response to immune checkpoint blockade. *JAMA Oncol.* 2019;5:471–478.

5. Halabi S, Kelly WK, Ma H, et al. Meta-analysis evaluating the impact of site of metastasis on overall survival in men with castration-resistant prostate cancer. *J Clin Oncol.* 2016;34:1652–1659.

6. Bubendorf L, Schopfer A, Wagner U, et al. Metastatic patterns of prostate cancer: an autopsy study of 1,589 patients. *Hum Pathol.* 2000;31:578–583.

7. Holmes MG, Foss E, Joseph G, et al. CT-guided bone biopsies in metastatic castration-resistant prostate cancer: factors predictive of maximum tumor yield. *J Vasc Interv Radiol.* 2017;28:1073–1081.e1.

8. Spritzer CE, Afonso PD, Vinson EN, et al. Bone marrow biopsy: RNA isolation with expression profiling in men with metastatic castration-resistant prostate cancer—factors affecting diagnostic success. *Radiology.* 2013;269:816–823.

9. McKay RR, Zukotynski KA, Werner L, et al. Imaging, procedural and clinical variables associated with tumor yield on bone biopsy in metastatic castration-resistant prostate cancer. *Prostate Cancer Prostatic Dis.* 2014;17:325–331.

10. Sailer V, Schiffman MH, Kossai M, et al. Bone biopsy protocol for advanced prostate cancer in the era of precision medicine. *Cancer.* 2018;124:1008–1015.

11. Coleman RE. Clinical features of metastatic bone disease and risk of skeletal morbidity. *Clin Cancer Res.* 2006;12:6243s–6249s.

12. Perera M, Papa N, Christidis D, et al. Sensitivity, specificity, and predictors of positive $^{68}$Ga-prostate-specific membrane antigen positron emission tomography in advanced prostate cancer: a systematic review and meta-analysis. *Eur Urol.* 2016;70:926–937.

13. Lecouvet FE, Oprea-Lager DE, Liu Y, et al. Use of modern imaging methods to facilitate trials of metastasis-directed therapy for oligometastatic disease in prostate cancer: a consensus recommendation from the EORTC Imaging Group. *Lancet Oncol.* 2018;19:e534–e545.

14. van Steenbergen TRF, Smits M, Scheenen TWJ, et al. $^{68}$Ga-PSMA-PET/CT and diffusion MRI targeting for cone-beam CT-guided bone biopsies of castration-resistant prostate cancer patients. *Cardiovasc Intervent Radiol.* 2020;43:147–154.

15. Bins S, Cirkel GA, Gadellaa-Van Hooijdonk CG, et al. Implementation of a multicenter biobanking collaboration for next-generation sequencing-based biomarker discovery based on fresh frozen pretreatment tumor tissue biopsies. *Oncologist.* 2017;22:33–40.

16. Boellaard R, Oyen WJG, Giammarile F, et al. FDG PET/CT: EANM procedure guidelines for tumour imaging: version 2.0. *Eur J Nucl Med Mol Imaging.* 2015;42:328–354.

17. Shamonin DP, Bron EE, Lelieveldt BP, et al. Fast parallel image registration on CPU and GPU for diagnostic classification of Alzheimer's disease. *Front Neuroinform.* 2014;7:50.

18. Klein S, Staring M, Murphy K, Viergever MA, Pluim JP. Elastix: a toolbox for intensity based medical image registration. *IEEE Trans Med Imaging.* 2010;29: 196–205.

19. Lowekamp BC, Chen DT, Ibáñez L, Blezek D. The design of SimpleITK. *Front Neuroinform.* 2013;7:45.

20. Chakravarty D, Gao J, Phillips SM, et al. OncoKB: a precision oncology knowledge base. *JCO Precis Oncol.* 2017;2017:10.1200/PO.17.00011.

21. Priestley P, Baber J, Lolkema MP, et al. Pan-cancer whole-genome analyses of metastatic solid tumours. *Nature.* 2019;575:210–216.

22. van Dessel LF, van Riet J, Smits M, et al. The genomic landscape of metastatic castration-resistant prostate cancers using whole genome sequencing reveals multiple distinct genotypes with potential clinical impact. *Nat Commun.* 2019; 10:5251.

23. Mermel CH, Schumacher SE, Hill B, Meyerson ML, Beroukhim R, Getz G. GISTIC2.0 facilitates sensitive and confident localization of the targets of focal somatic copy-number alteration in human cancers. *Genome Biol.* 2011;12:R41.

24. McLaren W, Gil L, Hunt SE, et al. The Ensembl Variant Effect Predictor. *Genome Biol.* 2016;17:122.

25. Harrow J, Frankish A, Gonzalez JM, et al. GENCODE: the reference human genome annotation for the ENCODE project. *Genome Res.* 2012;22:1760–1774.

26. Martincorena I, Raine KM, Gerstung M, et al. Universal patterns of selection in cancer and somatic tissues. *Cell.* 2017;171:1029–1041.e21.

27. The R Project for Statistical Computing website. https://www.r-project.org/. Accessed June 4, 2020.

28. van der Velden DL, Hoes LR, Van der Wijngaart H, et al. The drug rediscovery protocol facilitates the expanded use of existing anticancer drugs. *Nature.* 2019;574:127–131.

29. Paschalis A, Sheehan B, Riisnaes R, et al. Prostate-specific membrane antigen heterogeneity and DNA repair defects in prostate cancer. *Eur Urol.* 2019;76:469–478.

30. Wang B, Gao J, Zhang Q, et al. Diagnostic value of ^{68}Ga-PSMA PET/CT for detection of PTEN expression in prostate cancer: a pilot study. *J Nucl Med.* November 22, 2019 [Epub ahead of print].

31. Thang SP, Violet J, Sandhu S, et al. Poor outcomes for patients with metastatic castration-resistant prostate cancer with low prostate-specific membrane antigen (PSMA) expression deemed ineligible for ^{177}Lu-labelled PSMA radioligand therapy. *Eur Urol Oncol.* 2019;2:670–676.